Molecular Plant Advance Access published June 14, 2013

Microtubule depolymerization affects endocytosis and exocytosis in the tip and influences endosome movement in tobacco pollen tubes

Aurora Irene Idilli,[1] Piero Morandini,[1] Elisabetta Onelli,[1] Simona Rodighiero,[2] Marco Caccianiga[1] and Alessandra Moscatelli[1*]

[1] Department of Biosciences –Milan University, Via Celoria 26, Milan, Italy

[2] Fondazione Filerete –Milan University, Viale Ortles 22, Milan, Italy.

Running title: MT-dependent endocytosis in the pollen tube tip

Short summary: MTs are necessary to control exo-endocytosis in the tip. MTs depolymerization affects PM invagination in the apex and subsequent transport of endosomes for degradation. Moreover, MT dynamics influences the rate of exocytosis in the central domain of the tip.

*Corresponding author:
Alessandra Moscatelli
Department of Biosciences
University of Milan
Via Celoria 26, 20133 Milan (Italy)
e-mail: alessandra.moscatelli@unimi.it
Tel. +39-02-50314846
Fax +39-02-50314840

ABSTRACT

Polarized organization of the cytoplasm of growing pollen tubes is maintained by coordinated function of actin filaments (AFs) and microtubules (MTs). AFs convey post-Golgi secretory vesicles to the tip where some fuse with specific domains of the plasma membrane (PM). Secretory activity is balanced by PM retrieval that maintains cell membrane economy and regulates the polarized composition of the PM, by dividing lipids/proteins between the shank and the tip. Although AFs play a key role in PM internalization in the shank, the role of MTs in exo-endocytosis needs to be characterized.

The present results show that integrity of the MT cytoskeleton is necessary to control exo-endocytosis events in the tip. MT polymerization plays a role in promoting PM invagination in the apex of tobacco pollen tubes since Nocodazole affected PM internalization in the tip and subsequent migration of endocytic vesicles from the apex for degradation. MT depolymerization in the apex and shank was associated with misallocation of a significantly greater amount of internalized PM to the Golgi apparatus and its early recycling to the secretory pathway. FRAP experiments also showed that MT depolymerization in the tip region influenced the rate of exocytosis in the central domain of the apical PM.

Key words: pollen tube, microtubules, endocytosis, exocytosis

INTRODUCTION

Angiosperm pollen tubes are highly polarized cells that elongate in style transmitting tissue to transport sperm cells to the embryo sac for double fertilization. The mechanism of tip growth requires fast intense exocytosis in the apical flanks of the tube, where post-Golgi secretory vesicles (SVs) fuse, reversing external pectins for the construction new cell wall (Zonia and Munnik, 2008; Moscatelli et al., 2012; Chebli et al., 2012). As a consequence of this high secretory activity, membrane is secreted in the tip of growing pollen tubes in excess of that required for elongation, so that a mechanism of plasma membrane (PM) retrieval has been hypothesized to maintain cell membrane economy (Steer and Steer 1989). This mechanism of tip growth also provides specific sets of proteins that define a tip-growth domain having a specific PM protein/lipid content (Hepler et al., 2001; Kost et al., 1999; Potocky et al., 2003; Helling et al., 2006). As the pollen tube elongates, polarized PM protein composition which modulates the cell wall deposition (Cai et al. 2011; Chebli et al., 2012), also implies selective removal/ recycling of molecules between the shank and the tip PM (Moscatelli and Idilli, 2009; Onelli and Moscatelli, 2013).

Studies on endocytosis in pollen tubes have shown distinct internalization pathways involving the shank and surprisingly also the apical PM (Moscatelli et al., 2007; Zonia and Munnick, 2008). Time lapse experiments and ultrastructural studies using charged nanogold allowed to dissect the endocytic process and to show that PM internalized in the shank is mostly recycled to the secretory pathway and partially directed to vacuoles (Parton et al., 2001; Moscatelli et al., 2007; Zonia and Munnik, 2008; Bove et al., 2008). PM endocytosed in the apex is mostly conveyed to the degradation pathway and partly involved in a recycling process limited to the tip (Parton et al., 2001; Moscatelli et al., 2007). A mechanism of endocytosis in the tip was recently shown to be involved in recycling diacyl glycerol from the flanks to the tip of growing pollen tubes, thus regulating a differential lipid composition in the apical PM (Helling et al., 2006). Actin polymerization was suggested to promote endocytosis in the pollen tube shank, as Latrunculin B (LatB), a potent inhibitor of actin polymerization (Coué et al., 1987), affects internalization of PM destined for recycling and secretion through the Golgi apparatus, as well as that directed to vacuoles (Moscatelli et al. 2012). In contrast, PM internalized in the tip, which is also conveyed to vacuoles, appears to be actin-independent, further confirming the concept that distinct degradation pathways work in pollen tubes and raising doubts about the mechanism regulating PM internalization in the apex as well as endosome migration from this region to distal parts of the tube.

It was generally thought that the clear zone only contained SVs that accumulated and improved the secretory efficiency and were unable to make discrete movements apart

Brownian motion (Hepler et al., 2001). There is now evidence that endocytosis also occurs in the tip region and this suggests higher structural complexity. The clear zone is now considered to contain both SVs and endocytic vesicles. Moreover, internalization processes in the tip require directional movements to transport endocytic vesicles to vacuoles located behind the tip.

FRAP experiments carried out in the apical PM revealed another process requiring further investigation. Recent studies showed the complexity of the secretion map in pollen tube tip; in particular, actin-dependent fast secretion was demonstrated in the apical flanks of the tube. This secretion could be responsible for deposition of the cell wall material and slower, actin-independent exocytosis in the central domain of the apex (Moscatelli et al., 2012).

Although the role and importance of AFs in pollen tube cytoplasmic streaming and pollen tube growth are well established, the function of the MT cytoskeleton is still debated. The discovery of kinesin-immunoreactive homologues that associate with apical vesicles (Tiezzi et al., 1992; Cai et al., 1993; Liu et al., 1994), and promote MT sliding and organelle translocation in *in vitro* assays (Cai et al., 2000; Romagnoli et al., 2003), suggested that MTs could play a role in short-lived movements of membranes in pollen tubes.

In this study we examine the role of the MT apparatus in PM internalization in the shank and tip of growing pollen tubes, as well as endosome movements, by means of nocodazole (Noc), an anti-tumor agent that affects MT dynamic instability, leading to MT depolymerization *in vitro* and *in vivo* (Hoebeke et al., 1976; DeBrabander et al., 1976; Samson et al., 1979).

We show that MT depolymerization by 5 μM Noc influences membrane trafficking in the apex of tobacco pollen tubes. Time lapse internalization experiments and colocalization assays revealed that Noc affects PM internalization in the tip region and inhibits the migration of endocytic vesicles to the degradation pathway. Internalization experiments using negatively charged nanogold and colocalization assays in pollen tubes, transiently transformed with p-LAT52GFPRAB2 or p-LAT52GFPRABA4D and incubated with FM4-64, also showed that in the presence of Noc a greater amount of internalized PM is misallocated to Golgi apparatus and membrane trafficking in the tip is impaired. A further indication of the role of MTs in the apical region of the tube was derived from FRAP experiments with and without Noc. Although Noc had no effect on actin-dependent fast secretion occurring in the apical flanks, the rate of recovery of fluorescence in the central domain of the apex increased to the level of that of the apical flanks when MTs were inhibited. These data indicates that MTs control endocytosis in the tip region, are involved in endosome movement and regulate secretion in central domain of the tip.

RESULTS

Nocodazole affects microtubules in the apex and shank of tobacco pollen tubes

Recently, advances in plant molecular biology made it possible to observe protein localization and dynamics in living cells of stably or transiently transformed plant tissues. In an effort to check MT organization and dynamics in living pollen tubes, pollen grains were transiently transformed with two different constructs, in which GFP was fused with the *Arabidopsis* pollen-specific α-tubulin 1 isoform (TUA1) (Carpenter et al., 1992) and β-tubulin 6 isoform (TUB6) (Snustad et al., 1992) cDNAs (supplementary Fig. 1B, C). Our attempts to visualize MTs in live cells failed. Control experiments, carried out with pLAT52-GFPS65C, showed general diffuse fluorescence in the tube cytoplasm as well as in pollen tubes transformed with pLAT52-GFPTUA1 (supplementary Fig. 1D-E), suggesting that TUA1 was expressed but not incorporated into the MT arrays. Only when pLat52-GFPTUB6 was used were, discrete fluorescent aggregates observed in the cytoplasm. They occasionally seemed to be aligned along putative tracks (supplementary Fig. 1C, F). As our efforts to visualize MTs in live cells failed, the effect of DMSO or Noc on MT distribution was analyzed at different times by indirect immunofluorescence using an anti α-tubulin monoclonal antibody, as described.

Microtubule organization in control tubes proved similar to that already described in several plant species (n = 14 in three experiments) (Del Casino et al., 1993; Poulter et al., 2008; Gossot and Geitmann, 2007). MTs were organized as long, longitudinally oriented bundles in the older parts of the tube (up to 25-30 μm from tip PM) and as short randomly oriented strands in the shank and apex (Fig. 1A, yellow arrows). A similar arrangement was also observed in DMSO-treated tubes although short MT strands in the tip and shank appeared thicker after 15 min (Fig. 1B, yellow arrows) and the MT bundles seemed to extend through the shank, towards the apical region after 45 min incubation (Fig. 1C, yellow arrows). These data suggest that DMSO, known as polymerization agent of mammalian and pollen tubulin *in vitro* (Himes et al., 1977; Robinson and Engelborghs, 1982; Xu et al., 2005), also stabilizes MTs in tobacco pollen tubes. After treatment with 5 μM Noc for 15 and 45 min, MTs were completely depolymerized in the apex, where only fluorescent spots were still evident (Fig. 1D, white arrow). Moreover, MTs appeared more fragmented in the shank and the region characterized by short, randomly oriented MTs was more extensive in Noc-treated tubes, than in the control (Fig 1D, E, up to 40 and 60μm from the tip PM, respectively, see yellow

arrows). The use of 5 μM Noc therefore affected a subset of MTs localized in the apex and shank, while longitudinally oriented MT bundles in older parts of the tube, were unaffected.

Ultrastructural studies on pollen tubes after rapid freeze fixation and substitution have revealed an elaborate cytoskeleton comprising extensive networks of long actin cables and MTs throughout the shank, where they form an interconnected cortical system with the PM and elements of ER (Lancelle and Hepler 1991). Although it has been shown that MT depolymerization by Oryzalin does not alter AF organization (Poulter et al., 2008; Gossot and Geitmann, 2007), we tested for possible secondary effect of Noc on the distribution of AFs. The presence of Noc did not seem to affect their distribution; AFs are organized as longitudinally oriented bundles in the shank, whereas only diffuse staining has been observed in the tip where the actin cables are excluded (Lowy-Wheeler et al., 2005) (supplementary Fig. 2A-B). Frequently, thick bundle of short AFs, similar to the actin fringe already described in lily and tobacco pollen (Lowy-Wheeler et al., 2005) was observed in the apical flanks (supplementary Fig. 2A, arrows). Since the distribution of AFs in the apex and shank did not seem to be affected by Noc (supplementary Fig. 2C-D), any effects on endocytosis may be ascribed to MT depolymerization.

It is generally accepted that PM internalization has the main function of retrieving excess PM secreted during pollen tube growth (Steer and Steer 1989; Derksen et al. 1995). Although it is reported that treatment with the MT-disrupting drugs oryzalin and colchicine does not affect pollen tube growth (Laitiainen et al. 2002; Poulter et al., 2008; Gossot and Geitmann 2007), in order to exclude the possibility that Noc also does not impair pollen tube growth, pollen tubes incubated with DMSO or Noc were compared with those grown under control conditions (supplementary Fig. 3A-F). Measurements of tube length in two independent experiments showed that both DMSO and Noc induced a slight, sudden increase in growth rate, with respect to control after 15 min incubation, whereas after 45 min the growth rate of pollen tubes incubated with Noc decreased with respect to control (supplementary Fig. 3H, I). Statistical analysis revealed that the length of Noc-treated pollen tubes was not significantly different from that of pollen tubes incubated with DMSO after 15 min ($P = 0.733$ and $P = 0.937$ for experiments 1 and 2, respectively), whereas after 45 min the effect of Noc on pollen tube growth seemed more pronounced ($P = 0.0051$* and $P = 0.115$ for experiments 1 and 2, respectively).

Nocodazole affects plasma membrane internalization in the tip region and influences the timing of accumulation of V-shaped fluorescence

In tobacco pollen tubes, endocytosis involves at least two different PM domains, the shank (5-30 μm from tip) and the tip PM (the proximal 5 μm), leading to distinct endocytic pathways (Moscatelli et al. 2007).

In order to study the role of MTs in PM uptake in the tip and shank, time lapse internalization experiments were performed using lipophilic styryl dye FM4-64 (Bolte et al., 2004). Growing pollen tubes were incubated with DMSO or Noc for 15 min before the addition of FM4-64. The dynamics of internalization were recorded in specific areas of the cytoplasm: in the shank (5-30 μm from tip, Fig. 2A, BF purple and orange ROIs) and in the tip (the proximal 5 μm, Fig. 3A, BF green ROI) for 5 minutes. In general, the analyzed tubes displayed a variability in the level of PM internalization in the presence of both DMSO and Noc (Fig. 2C, D), as well as control tubes (Fig. 2B). Quantification and statistical analysis of ten tubes revealed that DMSO increased PM internalization in the apex, since the significantly different level of endocytosis between shank and apex, shown in control cells (Fig. 2B, $*P = 0.0018$, see Table 1) was abolished (Fig. 2C, $P = 0.95$, Table 1). When pollen tubes were incubated with Noc, internalization in the tip region significantly decreased with respect to the shank, thus restoring the ratio recorded in control tubes (Fig. 2D, $*P = 0.0128$, Table 1). Inhibition of MT polymerization therefore suggests that MTs could play a role in promoting PM internalization in the tip.

In control cells, internalized PM was recycled to the apex, to form the characteristic fluorescent inverted cone region (Parton et al. 2001; Moscatelli et al., 2007, Zonia and Munnik, 2008). In order to observe whether MT perturbation affected the distribution of endosomes or PM recycling, we traced the fate of internalized PM labelled with FM4-64. Pulsed chase experiments (FM4-64 incubated for 5 min) were carried out in pollen tubes in the presence of DMSO or Noc and fluorescence intensity was measured in the tip and shank of each tube at different times (see red and blue ROIs, respectively, in Fig. 3A, BF). Noc influenced the timing of fluorescence accumulation in the apex, since 5 min after removal of the dye, the fluorescence intensity ratio apex/shank of Noc-treated cells was significantly higher than in DMSO-treated cells ($*P = 0.0172$; Fig. 3A, C, E). This difference was no longer detected 15 and 30 min after FM4-64 removal (Fig. 3B, D, E). Moreover, statistical analysis showed that in the presence of DMSO the increase in fluorescence intensity in the tip region occurred gradually between 5 and 15 min ($*P = 0.0323$), whereas in the presence of Noc, the fluorescence intensity reached a plateau 5 min after removal of FM4-64 (Fig. 3E, and t-test in Table 2). The V-shaped accumulation of fluorescence in the tip was formed both by endocytic vesicles internalized in the apex and mostly directed to the degradation pathway and by membrane recycled to the secretory pathway (Moscatelli et al. 2007; Zonia and Munnik, 2008). Data from pulsed chase experiments suggested that the early increase of fluorescence intensity in the apex, in

the presence of Noc, could be due to endocytic vesicles, internalized in the tip region, whose movement toward the degradation pathway was delayed, to faster PM recycling to the secretory pathway and/or to change membrane trafficking in the tip.

Microtubule depolymerization delayed movement of endocytic vesicles from tip to shank

To verify the hypothesis that MT depolymerization impairs migration of endocytic vesicles from the tip region to the degradation pathway, we designed colocalization experiments with FM4-64 and Lysosensor Blue DND-167. Lysosensor is a fluorescent pH indicator with a pka of 5.1 that accumulates, as a result of protonation, in acidic compartments. This probe stains endosomes in the pollen tube shank (Moscatelli et al. 2007) and it also stained a set of vesicles in the pollen tube apex (Fig. 4A, D), suggesting that at least part of the vesicles in the clear zone could represent an early-endosome-like compartment. When pollen tubes were incubated with DMSO or Noc for 15 min before adding FM4-64 for another 15 min, images taken at 5, 15 and 30 min after removal of FM4-64 revealed colocalization in some areas of the V-shaped Lysosensor fluorescent domain and in the shank of DMSO- and Noc-treated cells (Fig. 4C, F). However, colocalization coefficients were significantly higher in Noc- than in DMSO-treated pollen tubes, after 5 min (*P = 0.0303) and 15 min (*P = 0.0160) (Fig. 4G and t-test in Table 3). After 30 min of incubation, the colocalization coefficients in Noc-treated tubes was still higher respect to cells incubated with DMSO but the difference was not significant (Fig. 4G, t-test in Table 3).

These results suggested that Lysosensor-positive compartments in the tip could represent an early sorting station for vesicles internalized in this region and that depolymerization of apical MTs delayed transport of newly internalized vesicles to the shank. However, the progressive increase in colocalization observed in DMSO-treated cells and the similar Pearson's coefficients of DMSO- and Noc-treated cells, 30 min after FM4-64 removal suggest that PM recycling could also increase the colocalization coefficient in time and that Noc improves PM recycling to the secretory pathway.

Nocodazole affects transport of negatively charged nanogold to vacuoles and induces misallocation of probe to Golgi apparatus

In our endocytosis experiments using negatively charged nanogold (Ng^-) and transmission electron microscopy to investigate the effect of Noc on internalization in the tip region, endocytosis dissection revealed that Ng^- was internalized in the apex and was mostly conveyed to vacuoles

without intersecting the Golgi apparatus or the secretory pathway (Moscatelli et al., 2007, Moscatelli et al., 2012).

In control assays, pollen tubes were incubated with DMSO for 15min and Ng^- was added and incubated for a further 30 min. Ng^- was observed in a limited number of vesicles in the tip region (Fig. 5A) and vesicles containing Ng^- (Fig. 5B, black arrows) were observed in close proximity of cortical MTs (Fig. 5B, white arrows) in the organelle-rich zone. In the presence of DMSO, the probe was directed along the degradation pathway because about 20% of vacuoles contained Ng^- after 30 min incubation (Table 4). Ng^- was never observed in stacks of Golgi bodies or Golgi-derived vesicles (Fig. 5C and Table 4).

In experiments in which pollen tubes were incubated with 5 μM Noc for 15 min before adding Ng^- and incubating for a further 30 min prior to fixation, electron microscope observations in the presence of Noc, showed that after 30 min the probe was present in a limited number of vesicles in the apex (Fig.5D, arrows). However, although a large number of cell sections were observed, the absence of whole apices and the limited number of tip regions did not enable us to confirm that endocytic vesicles internalized in the tip, accumulated in the clear zone in the presence of Noc. Besides, only 4.8% of vacuoles contained Ng^- after 30 min incubation (Table 4), suggesting that MTs were involved in the degradation pathway of PM internalized in the apex. Furthermore, MT depolymerization induced misallocation of probe to the Golgi apparatus (Fig. 5E, arrows). After 30 min incubation with Noc almost 21% of Golgi bodies contained Ng^- in the stacks and in Golgi-derived vesicles (Table 4). These results showed that MT depolymerization in the tip and shank induce misallocation of PM, internalized in the apex, to the Golgi apparatus.

Nocodazole induces recycling of a greater fraction of internalized plasma membrane to the Golgi apparatus and affects membrane trafficking in the tip

Colocalization experiments were carried out in pollen tubes transformed with pLAT52-GFPRAB2 (kind gift from A. Cheung, Department of Biochemistry and Molecular Biology, University of Massachusetts, Amherst, Massachusetts, USA) and FM4-64. Rab2 was shown to be expressed in the cis-face of Golgi apparatus (Cheung et al., 2002). As observed in other studies, the construct made it possible to visualize round organelles, having a mean area of 0.37 μm^2 (not shown), distributed in the shank and excluded from the clear zone (Fig. 6A, D). Transiently transformed pollen tubes pretreated with DMSO or Noc for 15 min, were incubated with FM4-64 for a further 15 min. Images taken at different times (5 min, 15 min and 30 min) after removal of the dye, showed that FM4-64 decorated the margins of fluorescent Golgi bodies in DMSO- and Noc-treated cells (Fig. 6A-C, D-F; white spots indicate colocalization points). Colocalization assays and

statistical analysis revealed significantly higher Pearson's coefficients in Noc– than DMSO-treated pollen tubes at all time points (Fig. 6A-C, D-F, G and Table 5), confirming that when the MT cytoskeleton is impaired in the apex and shank, a greater fraction of internalized PM is conveyed to the Golgi apparatus than in the control case.

In order to see if misallocation of tip-internalized PM to the Golgi apparatus induces further changes in the secretion pattern, we performed colocalization experiments in pollen tubes that transiently express the post-Golgi-associated vesicle protein RabA4d (Preuss et al. 2004; de Graaf et al. 2005; Szumlansky and Nielsen, 2009) .

Colocalization assays were performed in pollen tubes transiently transformed with the plasmid pUCLN /LAT52-GFPRABA4D (kindly donated by Dr A. L. Szumlanski and Prof. E. Nielsen, Department of Cellular and Developmental Biology, University of Michigan, Ann Arbor, Michigan USA). Approximately 5 hours after microprojectile bombardment, cells were incubated with DMSO or Noc for 15 min and then with FM4-64 for another 15 min. Images were taken 5, 15 and 30 min after removal of FM4-64. GFP-RabA4d- labelled vesicles were tip-localized and presented as highly dynamic small punctate structures in growing pollen tubes (Fig. 7A, D and movie 1 in supplemental material). Colocalization points, indicated by white spots, showed that the two signals did not completely overlap (Fig. 7C, F). Colocalization analysis performed in the apex and shank of the tube (whole) and Student's test on Pearson's coefficients showed that colocalization was higher in Noc-treated cells, 5 min (**P = 0.0097) and 15 min after removal of the dye (**P = 0.00070), whereas after 30 min it was similar in control and Noc-treated cells (P = 0.639) (Fig. 7C, F, G and Table 6), suggesting that MT depolymerization increases the speed of recycling. In order to see if MT depolymerization also affected the distribution of GFP-RabA4d-FM4-64-labelled vesicles, parallel colocalization analysis was carried out in the tip region (up to 10 μm from tip PM). Ratios between Pearson's coefficients of apex/whole (apex and shank) in single pollen tubes and Student's test revealed that although after 5 and 15 min the localization of GFP-RabA4d-FM464-labelled vesicles seemed to be more polarized in the apex of pollen tubes treated with DMSO, this difference was not significant (Fig. 7H, Table 6, t-test apex/whole). Moreover, after 30 min the distribution of GFP-RabA4d-FM464 vesicles was similar in control and Noc-treated tubes (Fig. 7H, Table 7, t-test apex/whole).

All these findings showed that MT depolymerization in the tip and shank affected endosome movement, improving PM transport to Golgi and impairing membrane trafficking in the tip region.

FRAP experiments showed that microtubules are involved in regulating secretion pattern in different domains of the apex

Our FRAP experiments using DMSO or Noc to determine whether MTs could also differentially affect secretion in different domains of the tip, included loading of FM4-64 in pollen tubes in the absence of DMSO and Noc for 5 min. The entire final 5 μm of apical PM of growing pollen tubes was bleached (Fig. 8A, E, green ROIs), while recovery was monitored in the central part of the tip (apex) (Fig. 8B, F; violet ROI) and in the apical flanks (Fig. 8B, F; orange and blue ROIs). Analysis of Mf in the presence of DMSO or Noc showed that PM fluorescence recovered to t^0 levels (before bleaching) in the apex and apical flanks (Fig. 8C, D and Fig. 8G, H). Statistical analysis performed on ten tubes for each experimental condition confirmed that recovery of the mobile fraction in the apex was not significantly different from that in the apical flanks (Fig. 8D, H, I). On the other hand, although the speed of fluorescence recovery was significantly higher in the apical flanks than in the apex in the presence of DMSO (Fig. 8D, L $*P = 0.018$ see Table 7), in Noc-treated pollen tubes, the speed of fluorescence recovery in the central region of the tip PM increased to that of apical flanks (Fig. 8H, I $P = 0.227$ see Table 7). Student's test showed that MT depolymerization significantly improved the rate of exocytosis in the central part of the apex respect to DMSO treated pollen tubes ($*P = 0.031$), suggesting that MTs could be involved also in regulating exocytosis in the central region of the tip (Table 7).

When we tested the effect of Noc on the diameter of pollen tube to see if loss of control of exocytosis in the central domain of the tip induced alterations in tube morphology, we found similar mean values for 45 min DMSO- and Noc treated pollen tubes (supplementary Fig. 4A) but a wider distribution of diameters with Noc than with DMSO (supplementary Fig. 4B, C, see also kurtosis values), suggesting that MTs could play a role in controlling pollen tube diameter.

A recent study showed that actin-dependent secretory activity also occurs in the pollen tube shank (Moscatelli et al., 2012), however the present FRAP experiments revealed that cortical MTs in the shank are not involved in exocytosis in this region, since the level and rate of fluorescence recovery were not affected (supplementary Fig. 5A-D).

Internalization of positively charged nanogold (Ng^+) was not affected by Nocodazole

In control cells, Ng^+ was internalized in the shank by CD and CI endocytosis. PM internalized by CD endocytosis, was recycled to secretory pathways through Golgi apparatus, whereas PM internalized by CI endocytosis was directed to vacuoles (Moscatelli et al., 2007). Internalization experiments performed with Ng^+ in the presence of DMSO or Noc showed that the probe was partly recycled to the secretory pathway through Golgi bodies, and conveyed to vacuoles in DMSO- and Noc-treated cells (Fig. 9A-D). However, quantification of stained Golgi bodies and vacuoles revealed that although the number of stained Golgi bodies was similar for control (DMSO-) and

Noc-treated pollen tubes, the number of vacuoles containing Ng^+ particles was slightly lower with Noc than for the control (Table 8). These findings suggest that although MT damage does not impair PM internalization in the shank, it may have a slight effect on transport towards the degradation pathway.

DISCUSSION

The present study provides data that assigns new roles to the MT cytoskeleton during pollen tube growth. Our results show that the integrity of the MT apparatus in the tip is critical for PM internalization in this region and for the subsequent transport of endosomes to the shank or for tip-localized membrane recycling. They enabled us to identify a new population of acidic vesicles in the clear zone that could be the first sorting station or early endosome for vesicles internalized in the tip region. As a consequence of endosome-defective transport from the tip to the shank, PM internalized in the apex is misallocated to Golgi apparatus. Moreover, since an increase of colocalization was also observed between internalized PM with RabA4d-positive vesicles it could be suggested that MT depolymerization induces changes in membrane sorting in the tip. Since MTs also appeared to regulate secretion in the central domain of the apical PM, cooperation could exist between AFs, which promote endocytosis in the shank and fast secretion in the apical flanks (Moscatelli et al., 2012), and MTs, which seem to play a key role in fine movements mostly occurring in the tip region.

Distinct effects of Nocodazole and oryzalin on the cytoskeletal apparatus and organelle distribution

In order to substantiate the role of MTs in PM internalization and/or endosome movement, we decided to employ nocodazole (Noc). Noc is known to inhibit tubulin polymerization *in vitro* (Hoebeke et al., 1976) and to induce reversible depolymerization of MTs *in vivo* and *in vitro*, at micromolar concentrations (De Brabander et al., 1976; Samson et al., 1979). More recently it was shown that Noc increases the rate of GTP hydrolysis in the E-site of the β-tubulin subunit (Mejillano et al., 1996) and significantly alters dynamic instability of MTs, increasing the time that MTs spend in pause and catastrophe frequency (Vasquez et al., 1997). In pollen tubes, Noc exerts its inhibitory effect on MTs in the apex and shank, without affecting the longitudinally oriented bundles in regions proximal to the granule.

Most of the studies on pollen tube MTs used the anti-MT drug oryzalin instead of Noc. Oryzalin is reported to have dramatic effects on all MT arrays, even at sub-micromolar

concentrations, leading to the loss of cytoplasmic zonation, with large organelles such as vacuoles, reaching the tip region (Joos et al., 1994). In order to substantiate our decision to use Noc, we performed experiments to test the effect of different concentration of Oryzalin on pollen tube growth and vacuole distribution. MTs were completely depolymerized after 15min incubation with 0.5μM Oryzalin (supplementary Fig. 6A). Moreover, a significant decrease in pollen tube elongation was observed after 45 min incubation with 0.5 μM Oryzalin in two independent experiments, with respect to control (supplementary Fig. 6C-D). On the other hand, although 0.1 μM Oryzalin completely depolymerized MTs along the whole tube (supplementary Fig. 6B), it did not inhibit pollen tube growth in two independent experiments (supplementary Fig. 6E-F).

Oryzalin 0.1 μM was used for further experiments. Vacuoles were imaged using Carboxy-CDFDA in live cells. Growing pollen tubes were incubated with the dye and then treated with Oryzalin, DMSO or Noc. Oryzalin affected the distribution pattern of vacuoles, since they were displaced toward the tip after 15 min (n = 19, in two experiments) and 30 min incubation (n = 15, in two experiments) (*P <0.05 and **P <0.001, respectively), respect to control (n= 27 two experiments) (supplementary Fig. 7A-B, E). Moreover, Oryzalin also induced lateral association of vacuoles, so altering cytoplasmic organization (supplementary Fig. 7A-B). The overall AF organization did not seem to be influenced by Oryzalin after 45 min incubation, although the fine organization of actin strands in the tip could not be observed (supplementary Fig. 2E-F).

On the contrary, DMSO (n = 20, two experiments) and Noc (n = 14, two experiments) did not affect the distribution pattern of vacuoles in the cytoplasm, respect to control (supplementary Fig. 7C-D, E).

Therefore, we think that 5 μM Nocodazole, that moderately affects MT polymerization in the apex and in the shank of the tube and minimizes the side effects on the cytoplasm organization, is preferable for prolonged studies (up to 45 min).

Tubulin polymerization facilitates PM invagination in the tip of growing pollen tubes

Attempts to observe MTs in live cells were not as many as those to visualize AFs. However, MTs were shown in tobacco pollen tubes transiently transformed with GFP-AtEB1 (Cheung et al., 2008). EB1 is known to be a plus end binding protein (Tirnauer et al., 2002) and further studies in somatic cultured cells showed that EB1 also bind with lower affinity the MT wall, giving typical comet-like structures (Chan et al., 2003). In tobacco pollen tubes EB1 was distributed along the whole surface of MTs and it is not clear yet whether it shows the whole MT apparatus or a subset of MTs (Cheung et al., 2008). EB1, as other heterologous MT-binding proteins binds to the Mt surface and could interfere with the constitutive organelle movements. To avoid this possibility, we decided to induce

in tobacco pollen tubes the transient expression of GFP-AtTUA1 or GFP-AtTUB6, which should have been incorporated in the MT lattice. The observation of MTs *in vivo* could allow us to check their polymerization state when we applied FM4-64 and to see endosomes moving on MT tracks. Unfortunately, our attempts were not successful; Although GFP-AtTUA1 and GFP-AtTUB6 were expressed in pollen tube they were not incorporated in the MT network and we had to show MTs by indirect immunofluorescence.

Inhibition of PM internalization in the tip region, induced us to question the mechanisms by which MT dynamics promotes PM invagination and internalization. For actin-dependent endocytosis, it is known that localized actin polymerization provides mechanical forces that favour PM curvature, vesicle scission and propulsion of nascent vesicles away from the PM (Schafer 2002) and that this process is under the control of RhoGTPase Arp2 ⁄ 3-based regulatory complex in animals and yeast (Soldati, 2003; Dawson et al., 2006). In pollen tubes, formins FH1 and FH3 localise in the shank PM and nucleate AFs (Cheung and Wu, 2004; Ye et al., 2009). Formin-based actin polymerization has therefore been postulated to deform the PM in the shank during endocytosis (Moscatelli et al., 2012).

The distribution pattern of MTs in control pollen tubes and the effects of Noc, suggest that dynamic MTs are present in the apical region, while more stable MTs, not influenced by the inhibitor, are organized in bundles in proximal regions. Studies to identify MT nucleation sites in pollen tubes revealed an immunoreactive homologue of a mammalian pericentriolar protein, associated with the apex and shank PM (Cai et al., 1996). These results suggest that localised polymerization of MTs, promoted by putative PM-associated MT-nucleating complexes, could facilitate PM deformation and internalization in the tip, as in the actin-dependent endocytosis. The negative effect of Noc on tubulin polymerization could therefore be responsible for the decreased endocytosis in this region. This hypothesis is further supported by the effect of DMSO on PM internalization in control assays. This solvent, which induces tubulin assembly (Sharma et al., 2007), seemed to promote tubulin polymerization in the apex and shank of the tube and to facilitate PM internalization in the tip.

Although most studies on pollen tube growth have been conducted *in vitro*, the implications of results for *in vivo* systems should also be considered. The MT-dependent internalization pathway in the tip region, mostly conveying to vacuoles, was postulated to be involved in internalization of a stigma-stylar Cys-rich adhesion protein (SCA) in lily pollen tubes (Kim et al., 2003). SCA is postulated to mediate pollen tube adhesion by binding a specific receptor in the tip PM (Kim et al., 2006), thus offering an example of receptor-mediated endocytosis, which confirmed the clathrin-

dependent mechanism of internalization in the apex (Zhao et al., 2010) and suggested an active role of MTs in mediating pollen tube-style molecular interactions *in vivo*.

The clear zone may represent the first sorting compartment for apically internalized PM in pollen tube

In plants the morphology of endosomes involved in degradation pathways is still debated, especially the nature of early endosomes. Endocytosis dissection experiments showed that of trans Golgi network (TGN) vesicles are the first compartment reached by $^{+}$Ng internalized in the shank of the tube and directed to vacuoles (Moscatelli et al., 2007). Negatively charged nanogold, which is internalized in the tip region, may have two different fates, namely the degradation pathway and tip-localized membrane recycling (Moscatelli et al., 2007). Colocalization assays using Lysosensor Blue and FM4-64 revealed acidic vesicles in the tip region, suggesting that they represent the first sorting compartment for apically internalized endocytic vesicles.

In animal cells, early endosomes appear as tubulovesicular organelles characterized by specific sets of Rab-GTPases (Gruenberg, 2001; Zerial and McBride, 2001). Although similar compartments have also been shown as the first sorting station of internalized $^{+}$Ng in tobacco protoplasts (Onelli et al., 2008), evidence of vacuolar H^{+}-ATPase activity in compartments of the trans Golgi network (TGN) suggested that this compartment can be regarded as an early endosome in plants (Dettmer et al., 2006). Further investigations also identified secretory carrier membrane protein isoform 1 (SCAMP1) as an integral proteins of trans Golgi tubular membranes and experiments showing colocalization with V-ATPase, confirmed that TGN represents the early endosome in BY-2 cells (Lam et al., 2007). The TGN appeared to be a highly dynamic and independent organelle, which only temporarily associated with Golgi stacks (Viotti et al., 2010) where endocytosis and exocytosis intersect, since the inhibition of an isoform of vacuolar H^{+}-ATPase causes accumulation of both endocytic and exocytic vesicles in the TGN. However, other studies on ECHIDNA mutants of *Arabidopsis thaliana*, in which certain TGN-resident proteins are misallocated, showed inhibition of exocytosis but not endocytosis, suggesting that these processes could be located in different TGN domains (Gendre et al., 2011).

Our demonstration of a population of acidic vesicles in the clear zone, together with recent data showing that the *Lilium* SCAMP1 isoform also localize in the clear zone in transiently transformed lily pollen tubes (Wang et al., 2010), suggest that endocytic vesicles destined for degradation or recycling to the PM could be sorted through distinct clear zone subdomains. However, further studies will be necessary to better characterize this compartment.

Microtubule depolymerization induces endosome misallocation and affects membrane trafficking in the tip

Although it was generally thought that only Brownian motions occurred in the clear zone (Hepler et al., 2001), the discovery of endocytic processes in the tip and movement of endosomes to the degradation pathway implied directional transports. Noc treatment showed that MT depolymerization delayed migration of endocytic vesicles from the clear zone to other destinations, namely the degradation pathway and/or apical recycling. Endocytosis dissection experiments with ¯Ng with and without Noc, suggested that at least part of the endocytic vesicles delayed in the clear zone could be directed to the degradation pathway, since a decrease in probe was seen in vacuoles in the presence of Noc. Moreover, the observation of ¯Ng-containing vesicles in close proximity with MTs in the shank, also suggested that MTs may be tracks for endocytic vesicles directed to the degradation pathway. Colocalization experiments in pollen tubes that transiently expressed GFP-Rab2, after FM4-64 internalization, showed that MT depolymerization induced misallocation of internalized PM to the Golgi.

Members of the Rab-GTPases family which are key players in membrane trafficking are present in the tip region of pollen tubes, where they regulate vesicle trafficking involved in exo- and endocytosis (Cheung and Wu, 2008). Among proteins that identify the trans-Golgi network (TGN), RabA4d is the *Arabidopsis* homolog of Rab11, which regulates polarized secretion and membrane trafficking in mammal and plant cells (Wilcke et al., 2000; Preuss et al. 2004; de Graaf et al. 2005; Szumlansky and Nielsen, 2009). In *Arabidopsis thaliana* and *Nicotiana tabacum* AtRabA4d/NtRAB11b resides on post-Golgi vesicles, including TGN, and may mediate exocytic trafficking. In both cases they have been associated with vesicles that accumulate in the tip region of growing pollen tubes (de Graaf et al., 2005; Szumlansky and Nielsen, 2009). Moreover, when a dominant negative mutant of NtRab11 is expressed in pollen tubes, internalized PM is not recycled to the secretory pathway, suggesting that NtRab11 could also be involved in endocytosis (de Graaf el al., 2005). Our colocalization results could suggest greater and faster recycling of internalized PM to the secretory pathway in the presence of Noc. This could be a consequence of misallocation of internalized PM and the greater amount of PM recycled to Golgi apparatus when the MT system is affected by Noc. However, the increase in recycling did not induce significant changes in pollen tube length at the times considered.

On the other hand, since RabA4d/NtRab11 seems also to play a role in recycling internalized PM (de Graaf el al., 2005), the increased colocalization of FM4-64 labelled membrane with RaA4D vesicles could be a consequence of impaired membrane recycling in the tip. Since Noc delayed the movement of tip-internalized endocytic vesicles toward the degradation pathway, it

could be otherwise hypothesized that MTs are involved in membrane sorting in the tip. Moreover, a role of MTs in vesicle transport has been suggested, using a monoclonal antibody against a neuronal kinesin that decorated MT-associated, tip-localized vesicles in tobacco pollen tubes (Tiezzi et al., 1991; Cai et al., 1993). On the other hand, Kif5B and Kifc1 have been shown to be involved in transport and fission of early endocytic vesicles along MTs in mouse liver cells (Nath et al., 2007).

Similarly to Lysosensor labeled compartments, vesicles revealed by GFP-RabA4d localized in the cytoplasm and accumulated in the tip region. Although it would be very interesting to determine whether or not RabA4d-labelled vesicles coincide with acidic vesicles shown by Lysosensor in the tip region, out attempts to load Lysosensor into transiently transformed pollen tubes were not successful.

Microtubule-dependent exocytosis in the central domain of the apical PM

It has been shown that PM internalized in the tip goes in at least two directions. Although a CD-dependent, MT-dependent internalization pathway has been shown for internalization of PM directed to vacuoles (Moscatelli et al., 2007; Moscatelli et al., 2012), we do not know whether internalization of PM destined for tip-localized recycling occurs by a different mechanism. In any case, we could postulate that endocytic vesicles internalized in the tip fuse with the first sorting compartment which occupy the clear, zone and then a sorting mechanism, addresses part of the internalized membrane to the degradation pathway and part to different regions of the apical PM. This tip-limited recycling process may not be involved in pollen tube growth but could take part in the redistribution of protein complexes or lipids between different membrane domains in order to maintain functional specialization in the apical PM.

Studies in the last few years have shown that secretory and endocytic pathways intersect in the apical clear zone of pollen tubes. These protein complexes may include factors involved in ionic regulation, such as Ca^{2+} channels, H^+ ATPases or K^+ and Cl^- transporters (Cheung and Wu, 2008), or in signal transduction, such as Rac/Rop GTPases. Phosphatidylinositol 4,5 biphosphate (PIP_2) is localized in the tip and seems to be directly involved in controlling actin–mediated targeted secretion, modifying membrane lipid composition and recruiting proteins involved in membrane fusion (Kost et al., 1999). PIP_2 is thus generated in the apex by PIP-kinase activity, and is hydrolyzed by phospholipase C 3 isoform in the apical flanks. In petunia, phospholipase C 1 isoform showed similar localization and helped restrict growth to the apex by regulating the distribution of PIP_2 (Dowd et al., 2006). Hydrolysis of PIP_2 results in the formation of 1,4,5 triphosphate and diacyl glycerol, which are both involved in controlling polarized growth, since diacyl glycerol is endocytosed at the edges of the apex and recycled to the central part of the apical

PM. Maintenance of asymmetrical distribution of these lipids is due to coordination of exocytic/endocytic processes.

The possibility that the apical sorting compartment could enable faster recycling of internalized PM limited to the tip is therefore intriguing and calls for further study.

Recently, FRAP experiments showed that although fast, actin-dependent exocytosis occurs in the apical flanks, slower actin-independent secretion occurs in the central part of the tip (Moscatelli et al., 2012). Results of the present study showed that slow exocytosis in the central domain of the apical PM is regulated by MT dynamics, since this process becomes as fast as that in the apical flanks in the presence of Noc. Slower exocytosis in the central area of the apex could therefore be part of the process, following sorting in the clear zone that regulates repositioning of signalling proteins, PLCs and lipids, in the apex. In the meantime it could have a role in recycling putative receptors to the PM for internalization by clathrin-dependent, receptor-mediated endocytosis in the apex (Zhao et al., 2010).

As a results of MT inhibition and changes in the pattern of exocytosis in the tip, we did not observe significant changes in pollen tube growth polarity. However, the analysis of tube diameters revealed a wider distribution of values in the presence of Noc, suggesting that MTs may play a role in the fine control of pollen tube diameter.

All these data highlight several lines of evidences and poses further questions. Among these, a central problem concerns MT-motor proteins that could be involved in promoting short-lived movements required to translocate newly internalized endocytic vesicles from the tip region to the degradation pathway or to reposition proteins / lipids in the apex.

In animal cells, MTs take part in endosome transport, cooperating with MT-motor proteins, such as kinesins and dyneins (Caviston and Holzbaur, 2006; Bryantseva and Zhapparova, 2012). In particular, the MT-kinesin system proved to have a role in receptor-ligand sorting in EEs in *in vitro* reconstitution experiments (Bananis et al., 2000). Kinesin homologs have been observed to accumulate in the tip region of growing pollen tubes of tobacco and *Pinus densiflora* (Tiezzi et al., 1992; Terasaka and Niitsu, 1994) and to be associated with Golgi-derived vesicles that interact with MT strands in the apex (Cai et al., 1993; Liu et al., 1994). However, although kinesin-related proteins have been shown to promote MT sliding and organelle movements on MTs in *in vitro* reconstituted assays (Cai et al., 2000; Romagnoli et al., 2003), further studies are needed to better identify the organelles with which kinesin-related proteins interact, in the pollen tube tip and how they could mediate directional movements in the apex and along the apical CD-dependent degradation pathway.

METHODS

Fluorescent probes and drugs

N-(3-triethylammoniumpropyl)-4-(p-diethylaminophenyl-hexatrienyl) pyridinium dibromide (FM4-64) (Invitrogen, USA) was dissolved in DMSO to a concentration of 16.4 mM and then diluted to 200 μM final concentration with distilled water. In time lapse assays and FRAP experiments the probe was used at 1 μM and in colocalization assays it was used at 4 μM in the culture medium. LysoSensor Blue DND-167 (Invitrogen, USA) was dissolved in DMSO to a concentration of 1 mM. In colocalization experiments this probe was used at 2 μM. Nocodazole (methyl 5-(2-thienylcarbonyl)-1Hbenzimidazol-2-yl) (Fluka, USA) stock solution in DMSO had a concentration of 10mM and was used in culture medium at a final dilution of 5 μM.

Pollen tube growth

Nicotiana tabacum (L.) pollen was collected from plants in the Botanical Garden (Cascina Rosa) of Milan University during summer and stored at -20°C. To measure pollen tube length and diameters transmission electron microscopy and immunolabelling, pollen grains were cultured in BK medium (Brewbaker and Kwack 1963) supplemented with 12% (w/v) sucrose at 23 ± 2°C as reported by Moscatelli et al. (2012). For in vivo time lapse experiments, one drop of pollen tube suspension (see above) was mixed with an equal amount of 1% low melting agarose (Sigma Aldrich, USA), dissolved in culture medium and stratified on polylysinated coverslips (2mg ml^{-1} polylysine for 2 hours). The growing pollen tubes were then overlayered with the medium and used for time lapse assays. For transient gene expression pollen grains were collected from fresh flowers of *Nicotiana tabacum* (L.) and allowed to germinate at 23°C on solid medium as reported by Kost et al. (1998).

Transient gene expression

Expression vectors were transferred to mature pollen grains on solid culture medium (see pollen tube growth) using a helium-driven particle accelerator (PDS-1000/He;Bio-Rad, Hercules, CA, USA). Pollen grains were placed under the stopping screen at a distance of 8 cm and bombarded in a vacuum of 28 inches of mercury using a helium pressure of 1100 psi, according to the manufacturer's recommendation (Bio-Rad) (Sanford et al., 1993). Tungsten particles (1 μm) were coated with plasmid DNA. Four micrograms of DNA was used to coat 1.5 mg of tungsten particles, which were used to bombard in two experiments (Kost et al., 1998) . Bombarded cells were kept at 23°C in the dark for 5 hours before observation.

Microtubule labelling

MTs were detected in pollen tubes grown in BK medium and then incubated in fixing solution, containing 3.7% formaldehyde, 10% sucrose, 100 mM Pipes, 5 mM MgSO4, 0.5 mM $CaCl_2$, 0.01% MBS pH 7.0. Noc (5μM) or DMSO (0.05%) or Oryzalin (0.1μM) was added to the fixing solution to prevent MT recovery during the early stages of fixation. Pollen tubes were rinsed twice with PEM buffer (50mM Pipes, 5mM EGTA, 1mM $MgCl_2$ pH 7.0) and treated for 2 min with 2% w/v cellulysin (Agar Scientific, UK) to partially digest the cell wall. After two rinses with PEM buffer, pollen tubes were treated with ice-cold methanol at -20°C for 3 min and rinsed twice with TBS (20 mM Tris, 150 mM NaCl, pH 7.5). They, were then incubated overnight with the anti-α tubulin primary monoclonal antibody B-5-1-2 (Sigma Aldrich, USA) diluted 1:200 in TBS and after two rinses with TBS, samples were incubated for 2 hours with FITC goat anti-mouse IgG (Invitrogen, USA) diluted 1:200 in TBS. Samples were finally rinsed with TBS and mounted using cytifluor (Agar Scientific, UK) and TBS. Optical sections (0.5 μm) and three-dimensional projections of specimens were obtained by the Leica TCS NT confocal microscope. A 40X objective was used for imaging. All images were recorded using a stepper motor to make Z-series.

Time lapse internalization experiments and quantitative analysis

Time lapse experiments were performed in live cells with a Leica TCS SP2 AOBS confocal microscope (Leica Microsystems GmbH, Wetzlar, Germany). FM4-64 was excited using the 488 nm laser line and FM4-64 fluorescence was imaged between 625 and 665 nm (Bolte et al., 2004). A 40X Leica oil immersion (NA 1.25) objective and a 2.7 zoom were used for all the experiments. Bright field imaging was performed with the transmitted light detector of the confocal microscope. To compare different experimental conditions, live data mode acquisitions were always performed with the same laser intensity and PMT settings. Viability of cells was assessed by recording pollen tube growth before addition of the dye, after incubation with 0.05% DMSO or 5 μM Noc for 15 min. Loading cells with the dye was achieved by direct addition of FM4-64 (1 μM) to liquid medium (containing DMSO or Noc) and time course recordings of FM4-64 uptake was carried out with the Leica TCS SP2 at 1 frame sec^{-1} for 250 sec. Observations were based on ten control, ten DMSO- and ten Noc-treated pollen tubes. Quantitative fluorescence analysis of FM4-64 internalization in the apex (up to 5μm from tip PM) and shank of the tube (5-25 μm from apical PM) was performed using the LCS software (Leica Microsystems, GmbH, Wetzlar, Germany). In more detail, forty frames after reaching the steady state fluorescence were considered and the mean fluorescence intensity in each region of interest (ROI) was calculated. Statistical analysis (paired Student's t-test) was done by Excel software.

Pulsed chase experiments using FM4-64 and fluorescence intensity analysis

For the pulsed chase experiments, pollen was germinated as reported in the previous section. Pollen tubes were incubated with DMSO or Noc before adding 1 μM FM4-64 for 5 min. After rinsing the dye, confocal images of pollen tubes (single medial sections) were taken after 5, 15 and 30 min by the Leica TCS SP2 confocal microscope. FM4-64 and bright field signals were imaged by 63X oil immersion (NA 1.4) objective (Leica Microsystems, GmbH, Wetzlar, Germany). The V-shaped fluorescence accumulation in the tip (Fig. 4A, BF, red ROI) and in the subapical region (Fig. 4A, BF, blue ROI) was monitored over time. Mean fluorescence intensity in the apex and in the subapical regions of single pollen tubes was calculated by ImageJ software (Rasband, W.S., ImageJ, U. S. National Institutes of Health, Bethesda, Maryland, USA, http://imagej.nih.gov/ij/, 1997-2012) (Schneider et al., 2012) and analysed by (Student's t-test) by the program Excel.

Colocalization experiments

For FM4-64–Lysosensor colocalization experiments, pollen tubes were germinated as reported for time lapse internalization experiments and quantitative analysis. Pollen tubes were incubated with LysoSensor Blue DND-167 2 μM for 30 min and the probe was removed before addition of 1 μM FM4-64 for 15 min. For FM4-64-pGFPRab2 and FM4-64-pGFPRabA4d colocalization experiments, pollen tubes on solid medium were incubated for 15 min with DMSO or Noc approximately 5 hours after projectile bombardment. Then 4 μM FM4-64 with DMSO/Noc was added to transiently transformed pollen tubes, on solid culture medium for 15 min. FM4-64–Lysosensor, pGFPRab2-FM4-64 and pGFPRabA4d-FM4-64 colocalization assays were carried out using the Leica TCS SP2 microscope with a 63X oil immersion (NA 1.4) objective (Leica Microsystems, GmbH, Wetzlar, Germany). The 488 nm and 561 laser lines were used to excite GFP and FM4-64 respectively. The fluorescence was collected in the following emission windows: 494-550 nm and 600-700 nm to acquire GFP and FM4-64 respectively. LysoSensor was excited with the 351 and 362 UV laser lines and the fluorescence emitted was collected between 400 and 490 nm. Images were recorded with the sequential scan mode of the LCS software (Leica Microsystems, GmbH, Wetzlar, Germany).

Colocalization analysis was carried out using the plug in JACoP of ImageJ software (Bolte and Cordelieres, 2006). The degree of colocalization was evaluated by calculating the Pearson's coefficient at different time points (Bolte and Cordelieres, 2006). For a visualization purpose, pixels with intensity values exceeding user-defined thresholds for both channels were represented as white spots in overlapped images (colocalized points):

For each experiment, Pearson's coefficients were calculated using the same ROI in all images.

Fluorescence recovery after photobleaching

For FRAP experiments, the pollen germination procedure was the same as for time lapse analysis. After recording pollen tube growth, FM4-64 was added to the cells for 15 min. Then FM4-64 was removed and the cells were rinsed three times with 0.5 ml liquid medium without the fluorochrome. Pollen tubes were then incubated for 15 min in medium with 0.05% DMSO or 5µM Noc. Five images of prebleached cells (t^0) were taken to confirm the stability of fluorescence in the sample. The central (apex) and lateral apical PMs (apical flanks) were then bleached (Figs. 9A a and 9B a show ROIs of bleaching) by intense illumination (AOTF 100%, zooming in the ROIs) with the 458, 476 and 488nm laser lines. FRAP was monitored using the 488 nm laser line and fluorescence was collected in the 625-665 nm emission window. Unprocessed data obtained as mean fluorescence values measured in the ROIs 2-4 during recovery were corrected from background (ROI 5 in Fig. 9A c) and spontaneous photobleaching (ROI 6 in Fig. 9A c). Fluorescence values obtained after correction were normalized with respect to fluorescence intensity before the photobleaching procedure.

Mobile fraction (Mf) and $t_{1/2}$ values were obtained by fitting the processed data with the following equation (Bulinski et al., 2001):

$$F_{(t)} = F_{max} - (F_{max} - F_{min}) e^{-t/\tau}$$

where $\mathbf{F_{max}}$ is fluorescence at steady state (prebleaching), $\mathbf{F_{min}}$ fluorescence just after photobleaching and $\boldsymbol{\tau}$ is the time constant.

The Mf is the percentage of molecules that diffuse to the bleached area:

$$Mf = \frac{(F_{max} - F_{min})}{(F_{max} - F_{min})}$$

and $t_{1/2}$ is:

$$t_{1/2} = \tau * \ln 2$$

Statistical analysis was performed by Student's t test.

Transmission electron microscopy

Pollen tubes grown for 60 min in BK medium (2.5 mg ml^{-1}) were incubated for 15 min with medium containing 0.05% DMSO or 5µM Noc (final dilution) before adding 30 nmol of positively or negatively charged nanogold particles (Nanoprobes, NY USA), resuspended in 200 µl distilled water (MilliQ grade). Samples with DMSO or Noc-treated cells were taken after 30 or 60 min and processed for fixation by the protocol reported in Moscatelli et al. (2007). Seventy nm ultra-thin sections, obtained using a Reichert Jung Ultracut E microtome, were collected on formvar-carbon coated nickel grids. Positively and negatively charged nanogold were enhanced with QH silver

(Nanoprobes, NY USA) for 2 min as described by the manufacturer. Sections were then stained with 3% (w/v) uranyl-acetate for 30 min and observed using an EFTEM LEO 912AB transmission electron microscope (Zeiss, Jena, Germany) operating at 80 kV.

ACKNOWLEDGEMENTS

We thank Dr T. Resch and Prof. A. Touraev (Max F. Perutz Laboratories, Department of Plant Molecular Biology, Vienna University), Prof. T. Hashimoto (Graduate School of Biological Sciences Nara Institute of Science and Technology, Ikoma, Japan), Dr A. Szulamski and Prof. E. Nilsen (Department of Molecular, Cellular and Development Biology, University of Michigan, USA) and Prof. A. Cheung (Department of Biochemistry and Molecular Biology, University of Massachusetts, Amherst, Massachusetts, USA), for providing p-LAT52-GFP, p-GFP-TUB6, p-LAT52-GFPRABA4D and p-LAT52-GFPRAB2, respectively.

Many thanks to Prof. Benedikt Kost, (Department of Biology, University of Erlangen-Nuremberg, Germany) for teaching us the procedures to perform successful and reproducible transient transformation experiments in tobacco pollen tubes.

We thank Dr Nadia Santo (CIMA) for technical assistance with the transmission electron microscope. Many thanks also to Dr Enrico Sala and Valerio Parravicini for taking care of tobacco plants and Roberto Cavatorta for photographic support.

This work was supported by the PRIN project 2008, financed by the Italian Ministry of Education.

FIGURE LEGENDS

Figure 1. Effects of 5 μM Noc on the MT cytoskeleton. (A) In control cells, MTs are organized as long, longitudinally oriented bundles in the older parts of the tube and as short, randomly oriented fragments in the apex and shank of the tube (yellow arrows). **(B-C)** In the presence of DMSO, short MT strands in the tip and in the shank appeared thicker after 15min incubation (B, yellow arrows). After 45min incubation, the region displaying MT bundles appeared to extend further towards the apex (yellow arrows). **(D-E)** Changes in MT cytoskeletal distribution were observed. In the presence of Noc; MTs in the tip region were completely depolymerized after 15 and 45 min incubation since only fluorescent spots were observed (white arrows) and the region occupied by MT fragments was more extensive than in control and DMSO-treated tubes (yellow arrows). Scale bar, 10 μm.

Figure 2. Time-lapse experiments using FM4-64 with and without 5 μM Noc. (A) A representative Noc-treated pollen tube at the beginning of recording. Coloured areas in the Bright Field (BF) image indicate regions in which fluorescence was measured. Green ROI indicates the area measured in the tip region, orange and violet ROIs indicate areas measured on the shank. **(B-D)** Graphs show mean fluorescence at the tip and in the shank of control tubes (B), pollen tubes treated with DMSO (C) or with Noc (D). Quantitative analysis of FM4-64 internalization in the apex and shank was performed considering the last 40 frames after steady state fluorescence was reached. Statistical analysis showed that Noc induced a significant decrease in PM internalization in the tip of tubes. Error bars indicate 67% confidence intervals (n = 10). The resolution of confocal images was. Scale bar, 10 μm.

Figure 3. Time course of FM4-64-labelled PM accumulation in the tip region. (A-D) Medial plane images of pollen tubes 5 and 30 min after FM4-64 loading, with or without Noc. Coloured areas in BF image indicate regions in which fluorescence was measured (A, BF). Red ROI indicates area measured in the apex, blue ROI indicates area measured in the subapical region. **(A-B, F)** In the presence of DMSO, accumulation of fluorescence in the tip was slower and less than in cells incubated with Noc. Statistical analysis of the ratio of mean fluorescence of the apical to subapical ROIs showed that in the presence of DMSO fluorescence intensity in the tip region significantly increased between 5 and 15 min (F), whereas with Noc, it was similar 5 and 15 min after FM4-64 removal (C-D, F). A significant difference in the tip fluorescence intensity was also recorded between DMSO- and Noc-treated tubes, 5 min after FM4-64 removal. Error bars indicate 67% confidence intervals (n = 8 and n = 10 for DMSO and Noc treated cells). Scale bar, 10 μm.

Figure 4. Colocalization analysis with Lysosensor Blue DND-167 and FM4-64. (A-C) Lysosensor detected a cluster of acid vesicles accumulating in the tip region of pollen tube cells (A). The cluster did not completely overlap with FM4-64 fluorescent vesicles in the clear zone (B). White spots show colocalization points in the presence of DMSO (C). **(D-F)** An increase in colocalization of Lysosensor- (D) and FM4-64-labelled vesicles (E) was observed with Noc (F, white spots). **(G)** Statistical analysis of Pearson's coefficients in the presence of DMSO and Noc at different times showed that Noc induced a significant increase in colocalization of newly internalized apical vesicles after 5 and 15 min after removal of the dye. After 30 min with Noc, the colocalization coefficient was even higher respect to DMSO-treated pollen tubes. Error bars indicate 67% confidence intervals (n = 7).Scale bar, 10 μm.

Figure 5. Internalization of negatively charged nanogold in DMSO- and Noc-treated pollen tubes. (A) In the presence of DMSO, negatively charged nanogold was internalized in the clear zone. Numerous endocytic vesicles, containing the probe, are evident close to the apical PM CW indicates the cell wall. Scale bar, 500nm. **(B)** Endosomes containing negatively charged nanogold particles (black arrows) are evident in close contiguity with cortical MTs (white arrows) in DMSO-treated cells, after 30 min incubation with the probe. Scale bar, 100 nm. **(C)** Golgi bodies (G) were not involved in transport of negatively charged nanogold in the presence of DMSO. Scale bar, 200 nm. **(D)** Internalization of negatively charged nanogold was observed in a limited number of vesicles near the apical PM in the presence of Noc. Scale bar, 500 nm. **(E)** In the presence of Noc the probe was misallocated to Golgi apparatus (G, black arrows). Scale bar, 200 nm.

Figure 6. Colocalization experiments with FM4-64 in p-LAT52-GFPRAB2-transformed pollen tubes

(A-C) The fusion protein GFP-Rab2 allowed us to show Golgi bodies that are localized in the pollen tube cytoplasm but excluded from the tip region (A), where FM4-64 labelled vesicles accumulated to form the typical inverted cone region (B). White spots showed colocalization points in the presence of DMSO (C). **(D-F)** In the presence of Noc an increase in colocalization of Golgi bodies (D) and FM4-64 was observed (F, the white spots, showing the colocalization points, highlight the margins of Golgi cisternae). **(G)** Statistical analysis considering Pearson's coefficients in the presence of DMSO and Noc at different times showed that Noc induceed a significant increase in colocalization of internalized PM and Golgi apparatus 5 and 30 min after removal of the fluorochrome. Error bars indicate 67% confidence intervals (n = 11). Scale bar, 10 μm.

Figure 7. Colocalization experiments with FM4-64 in p-LAT52-GFPRABA4D transformed pollen tubes.

(A-C) GFP-RabA4d was associated with vesicles distributed along the tube and concentrating in the tip (A), where FM4-64-labelled membranes also accumulated (B). White spots showed colocalization points in the presence of DMSO (C). **(D-F)** In the presence of Noc an increase in colocalization of RabA4d-compartments (D) and FM4-64 was observed (F, white spots show colocalization points). **(G)** Statistical analysis considering Pearson's coefficients in the presence of DMSO and Noc at different times showed that Noc induced a significant increase in colocalization of internalized PM with RabA4d-vesicles 5 and 15 min after removal of the fluorochrome, while at 30 min the colocalization coefficient with Noc was not significantly higher than in DMSO-treated cells. **(H)** The ratio of Pearson's coefficients in the apex to those measured in the apex and shank (whole) at different times showed that MT depolymerisation did not significantly affect the position of colocalization points in DMSO- and Noc-treated cells. Error bars indicate 67% confidence intervals (n = 8). Scale bar, 10 μm.

Figure 8. FRAP analysis in the apical PM in the presence of DMSO or Noc. The whole apical PM was bleached **(A)**, (green ROI, DMSO t^0) and recovery was monitored in the tip **(B)** (violet ROI), and apical flanks of PM **(B)** (orange and blue ROIs), until recovery was complete, 62 frames post-bleaching (62F PB) **(C)**. No difference in the amount of fluorescence recovered in the lateral and central part of the apical PM was observed in DMSO treated pollen tubes compared to before bleaching (t^0) **(D, I)**. On the contrary, the rate of recovery in the apical flanks of the PM was significantly higher than in the apex **(D, L)**. In Noc-treated pollen tubes, FRAP experiments using the same set up as for the control (DMSO) **(E-G)** showed that although Noc did not affect the Mf **(H, I)**, differences in the rate of recovery of the various domains of the apical PM disappeared **(H, L)**. **(D, H)** Each time point in the plots represents the mean of all the cells analysed (GRAPHPAD, PRISM 4 software). **(I, L)** Bar diagram outcomes of statistical analysis comparing data of Mf and t1⁄2 calculated by the fitting individual experiments (n = 10). Although Noc did not influence fluorescence recovery (Mf) **(I)**, it significantly increased the speed of fluorescence recovery in the central domain of the apical PM **(L)**. Error bars indicate 67% confidence intervals (n = 10). Scale bar, 5 μm.

Figure 9. Internalization of positively charged nanogold in DMSO- and Noc-treated pollen tubes

In DMSO- and Noc-treated pollen tubes positively charged nanogold was delivered to vacuoles **(A, B** black arrows**)** and Golgi apparatus **(A** white arrows**, C, D** black arrows**).** Scale bar 200 nm.

TABLES

Table 1 PM internalization paired Student's test	
Co apex vs Co shank	*P* = **0.0018***
DMSO apex vs DMSO shank	*P* = 0.954
Noc apex vs Noc shank	*P* = **0.0128***
For the statistical analysis, ten cells have been considered in Coontrol, in DMSO and in Noc treated cells	

Table 2 Ratio fluorescence intensity Student's test	
DMSO 5 min vs Noc 5 min	*P* = **0.0172***
DMSO 15 min vs Noc 15 min	*P* = 0.255
DMSO 45 min vs Noc 30 min	*P* = 0.431
DMSO 5 min vs DMSO 15 min	*P* = **0.0.0323***
Noc 5min vs Noc 15 min	*P* = 0.788
For the statistical analysis, eight and ten cells have been considered at each time, in DMSO and in Noc treated cells, respectively	

Table 3 Colocalization Lysosensor-FM4-64 Student's test	
DMSO 5 min vs Noc 5 min	*P* = **0.0303***
DMSO 15 min vs Noc 15 min	*P* = **0.0160***
DMSO 30 min vs Noc 30 min	*P* = 0.140
For the statistical analysis, almost seven cells have been considered, at each time, in DMSO and in Noc treated cells	

Table 4 Percentage of stained compartments with negatively charged nanogold		
	N. of vacuoles	**stained**
30 min DMSO	135	20.7%
30 min Noc	415	4.8%
	N. of Golgi	**stained**
30 min DMSO	21	0
30 min Noc	78	21.8%
For quantification, 100 cell sections were considered for DMSO and Noc treated cells		

Table 5 Colocalization Rab2-FM4-64 Student's test	
DMSO 5 min vs Noc 5 min	*P* = **0,019***
DMSO 15 min vs Noc 15 min	*P* = **0.0004****
DMSO 30 min vs Noc 30 min	*P* = **0.024***
For the statistical analysis, almost 11 cells have been considered, at each time, in DMSO and Noc treated tubes	

Table 6 Colocalization RabA4d-FM4-64 Student's test whole (apex and shank)	
DMSO 5 min vs Noc 5 min	*P* = **0.0097****
DMSO 15 min vs Noc 15 min	*P* = **0.0007****
DMSO 30 min vs Noc 30 min	*P* = 0.639
For the statistical analysis, almost 8 cells have been considered, at each time in DMSO and Noc treated tubes	

Table 7 FRAP experiments Student's test t1/2	
DMSO apex vs apical flanks	P = **0.018***
Noc apex vs apical flanks	P = 0.227
DMSO vs Noc apex	P = **0.031***

For the statistical analysis, almost 10 cells have been onsidered, in DMSO and Noc treated tubes

Table 8 Percentage of stained compartments with positively charged nanogold		
	N. of vacuoles	**stained**
30 min DMSO	81	74%
30 min Noc	196	60.2%
	N. of Golgi	**stained**
30 min DMSO	47	91.5%
30 min Noc	36	97.2%

For quantification, 100 cell sections were considered for DMSO and Noc treated cells

REFERENCES

Bananis, E., Murray, J.W., Stockert, R.J., Satir, P., and Wolkoff, A.W. (2000). Microtubule and motor-dependent endocytic vesicle sorting in vitro. J. Cell Biol. **151**, 179-186.

Bolte, S., Talbot, C., Boutte, Y., Catrice, O., Read, N.D., and Satiat-Juenemaitre, B. (2004). FM-dyes as experimental probes for dissecting vesicle trafficking in living plant cells. J. Microsc. **214**, 159-173.

Bolte, S., and Cordelier, F.P. (2006). A guided tour into subcellular colocalization analysis in light microscopy. J. Microsc. **224**, 213-232.

Bove, J., Vaillancourt, B., Kroeger, J., Hepler, P.K., Wiseman, P.W., and Geitmann, A. (2008). Magnitude and direction of vesicle dynamics in growing pollen tubes using spatiotemporal image correlation spectroscopy and fluorescence recovery after photobleaching. Plant Physiol. **147**, 1646-1658.

Brewbaker, J.L., and Kwack, B.H. (1963). The essential role of calcium ions in pollen germination and pollen tube growth. Am. J. Bot. **50**, 859-865.

Bryantseva S.A., and Zhapparova O.N. (2012) Bidirectional transport of organelles: unity and struggle of opposing motors. Cell Biol. Int. **36**, 1-6.

Bulinski, J.C., Odde, D.J., Howell, B.J., Salmon, T. D., and Waterman-Storer, C.M. (2001). Rapid dynamics of the microtubule binding of ensconsin in vivo. J. Cell Sci. **114**, 3885-3897.

Cai, G., Bartalesi, A., Del Casino, C., Moscatelli, A., Tiezzi, A., and Cresti, M. (1993). The kinesin - immunoreactive homologue from *Nicotiana tabacum* pollen tubes: Biochemical properties and subcellular localization. Planta **191**, 496-506.

Cai, G., Moscatelli, A., Del Casino, C., Chevrier, V., Mazzi, M., Tiezzi, A., and Cresti M. (1996). The anti-centrosome monoclonal antibody 6C6 reacts with a plasma membrane-associated polypeptide of 77 kDa from *Nicotiana tabacum* pollen tubes. Protoplasma **190**, 68-78.

Cai, G., Romagnoli, S., Moscatelli, A., Ovidi, E., Gambellini, G., Tiezzi, A., and Cresti, M. (2000). Identification and characterization of a novel microtubule-based motor associated with membranous organelles in tobacco pollen tubes. Plant Cell **12**, 1719-1736.

Cai, G., Faleri, C., Del Casino, C., Emons, A.M.C., and Cresti, M. (2011). Distribution of callose synthase and sucrose synthase in tabacco pollen tube is controlled in dissimilar ways by actin filaments and microtubules. Plant Physiol. **155**, 1169-1190.

Carpenter, J.L., Ploense, S.E., Snustad, D.P., and Silflow, C.D. (1992). Preferential expression of an α-tubulin gene of *Arabidopsis* in pollen. Plant Cell **4**, 557-571.

Caviston, J.P., and Holzbaur, E.L.F. (2006). Microtubule motors at the intersection of trafficking and transport. Trends Cell Biol. **16**, 530-537.

Chan, J., Calder, G.M., Doonan, J.H., and Lloyd, C.W. (2003). EB1 reveals mobile microtubule nucleation sites in *Arabidopsis*. Nat. Cell Biol. **5**, 967-971.

Chebli, Y., Kaneda, M., Zerzour, R., and Geitmann, A. (2012). The cell wall of the *Arabidopsis* pollen tube-spatial distribution, recycling and network formation of polysaccharides. Plant Physiol. **160**, 1940-1955.

Cheung, A. Chen, C. Y.H., Glaven, R. H., de Graaf, B. H. J., Vidali, L., Hepler, P. K., and Wu, H-M. (2002). Rab2 GTPase regulates vesicle trafficking between the endoplasmic reticulum and the Golgi bodies and is important to pollen tube growth. Plant Cell **14**, 945-962.

Cheung, A.Y., and Wu, H.M. (2004). Overexpression of an *Arabidopsis* formin stimulates supernumerary actin cable formation from pollen tube cell membranes. Plant Cell **16**, 257-269.

Cheung, A.Y., and Wu, H. (2008). Structural and signaling networks for the polar cell growth machinery in pollen tubes. Annu. Rev. Plant Biol. **59**, 547-572.

Cheung, A.Y., Duana, Q-H., Santos Costad, S., de Graaf, B.H.J., Di Stilio, V.S., Feijo, J., and Wu, H-M. (2008). The dynamic pollen tube cytoskeleton: live cell studies using actin-binding and microtubule-binding reporter proteins. Mol. Plant **1**, 686-702.

Coue´, M., Brenner, S.L., Spector, I., and Corn, E.D. (1987). Inhibition of actin polymerization by latrunculin A. FEBS Letters. **213**, 316-318.

Dawson, J.C., Legg, J.A., and Manchesky, L.M. (2006). Bar domain proteins: a role in tabulation, scission and actin assembly in clathrin-mediated endocytosis. Trends Cell Biol. **16**, 493-498.

de Graaf, B.H., Cheung, A.Y., Andreyeva, T., Levasseur, K., Kieliszewski, M., and Wu, H. M. (2005). Rab11 GTPase-regulated membrane trafficking is crucial for tip-focused pollen tube growth in tobacco. Plant Cell **17**, 2564-2579.

DeBrabander, M.J., Van de Veire, R.M. L., Aerts, F.E. M., Borgers, M., and Jannsen, P.A. (1976). The effects of methyl [5-(2-thienylcarbonyl)-1H-benzimidazol-2-yl] carbamate (R 17,943: NSC 238159), a new synthetic antitumoral drug interfering with microtubules, on mammalian cells cultured in vitro. Cancer Res. **36**, 905-916.

Del Casino, C., Li, Y-Q., Moscatelli, A., Scali, M. and Tiezzi, A., and Cresti M. (1993). Distribution of microtubules during the growth of tobacco pollen tubes. Biol. Cell **79**, 125-132.

Derksen, J., Rutten, T., Lichtscheidl, I. K., Dewin, A. H. N., Pierson, E. S., and Rongen, G. (1995). Quantitative analysis of the distribution of organelles in tobacco pollen tubes: implication for exocytosis and endocytosis. Protoplasma **188**, 267-276.

Dettmer, J., Hong-Hermesdorf, A., Stierhof, Y. D., and Schumacher, K. (2006). Vacuolar H^+ATPase activity is required for endocytic and secretory trafficking in *Arabidopsis*. Plant Cell **18**, 715-730.

Dowd, P.E., Coursol, S., Skirpan, A.L., Kao, T.H., and Gilroy, S. (2006). Petunia phospholipase C1 is involved in pollen tube growth. Plant Cell **18**, 1438-1453.

Gendre, D., Oh, J.; Boutté, Y., Best, J. G., Samuels, L., Nilsson, R., Uemura, T., Marchant, A. Bennett, M. J. Grebe, M., and Bhalerao, R. P. (2011). Conserved *Arabidopsis* ECHIDNA protein mediates trans-Golgi-network trafficking and cell elongation. Proc. Natl. Acad. Sci. U S A **108**, 8048-8053.

Gossot, O., and Geitmann, A. (2007). Pollen tube growth: coping with mechanical obstacles involves the cytoskeleton. Planta **226**, 405-416.

Gruenberg, J. (2001). The endocytic pathway: a mosaic of domains. Nat. Rev. **2**, 721-730.

Helling, D., Possart, A., Cottier, S., Klahre, U., and Kost, B. (2006). Pollen tube tip growth depends on plasma membrane polarization mediated by tobacco PLC3 activity and endocytic membrane recycling. Plant Cell **18**, 3519-3534.

Hepler, P.K., Vidali, L., and Cheung, A.Y. (2001). Polarized cell growth in higher plants. Annu. Rev. Cell Dev. Biol. **17**, 159-187.

Hoebeke, J., Van Nijen, G., and DeBrabander, M. (1976). Interactions of oncodazole (R 17934), a new anti-tumoral drug, with rat brain tubulin. Biochem. Biophys. Res. Commun. **69**, 319-324.

Joos, U, van Aken, J., and Kristen, U. (1994). Microtubules are involved in maintaining the cellular polarity in pollen tubes of *Nicotiana sylvestris*. Protoplasma **179**, 5-15.

Kim, S.T., Mollet, J.C., Dong, J., Zhang, K., Park, S.Y., and Lord, E.M. (2003). Chemocyanin, a small, basic protein from the lily stigma, induces pollen tube chemotropism. Proceed. Nat. Acad. Sci. USA **100**, 16125-16130.

Kim, S.T., Kangling, Z., Dong, J., and Lord, E.M. (2006). Exogenous free ubiquitin enhances lily pollen tube adhesion to an in vitro stylar matrix and may facilitate endocytosis of SCA. Plant Physiol. **142**, 1397-1411.

Kost, B., Spielhofer, P., and Chua, N-H. (1998). A GFP-mouse talin fusion protein labels plant actin filaments *in vivo* and visualizes the actin cytoskeleton in growing pollen tubes. Plant J. **16**, 393-401.

Kost, B., Lemichez, E., Spielhofer, P., Hong, Y., Tolias, K., Carpenter, C., and Chua, N-H. (1999). Rac homologues and compartmentalized phosphatidylinositol 4,5-biphosphate act in a common pathway to regulate pollen tube growth. J. Cell Biol. **19**, 317-330.

Laitiainen, E., Nieminen, K.M., Vihinen, H., and Raudaskoski, M. (2002). Movement of generative cell and vegetative nucleus in tobacco pollen tubes is dependent on microtubule cytoskeleton but independent of the synthesis of callose plugs. Sex. Plant Reprod. **15**, 195-204.

Lam, S. K., Siu, C.,L., Hillmer, S., Jang, S., An, G., Robinson, D.G., and Jiang, L. (2007). Rice SCAMP1 defines clathrin coated, trans Golgi-located tubular-vesicular structures as an early endosome in tobacco BY-2 cells. Plant Cell **19**, 296-319.

Lancelle, S.A., and Hepler, P.K. (1991). Association of actin with cortical microtubules revealed by mmunogold localization in *Nicotiana* pollen tubes. Protoplasma **165**, 167–172.

Liu, G.Q., Cai, G., Del Casino, C., Tiezzi, A., and Cresti, M. (1994). Kinesin-related polypeptide is associated with vesicles from *Corylus avellana* pollen. Cell Motil. Cytoskel. **29**, 155-166

Lovy-Wheeler A., Wilsen K.L., Baskin, T.I., and Hepler, P.K. (2005). Enhanced fixation reveals the apical cortical fringe of actin filaments as a consistent feature if the pollen tube. Planta **221**, 95-104.

Mejillano, M.R., Shivanna, B.D., and Himes, R. (1996). Studies on the nocodazole-induced GTPase activity of tubulin. Arch. Biochem. Biophys. **336**, 130-138.

Moscatelli, A., Ciampolini, F., Rodighiero, S., Onelli, E., Cresti, M., Santo, N., and Idilli, A. (2007). Distinct endocytic pathways identified in tobacco pollen tubes using charged nanogold. J Cell Sci. **120**, 3804-3819.

Moscatelli, A., and Idilli, A.I. (2009). Pollen tube growth: a delicate equilibrium between secretory and endocytic pathways. J. Integr. Plant Biol. **51**, 727-739.

Moscatelli, A., Idilli, A.I., Rodighiero, S., and Caccianiga, M. (2012). Inhibition of actin polymerisation by low concentration Latrunculin B affects endocytosis and alters exocytosis in shank and tip of tobacco pollen tubes. Plant Biol. **14**, 770-782.

Nath, S., Bananis, E., Sarkar, S., Stockert, R.J., Sperry, A.O., Murray, J.W., and Wolkoff, A.W. (2007). Kif5B and Kifc1 interact and are required for motility and fission of early endocytic vesicles in mouse liver. Mol. Biol. Cell **18**, 1839-1849.

Onelli, E., Prescianotto-Baschong, C., Caccianiga, M., and Moscatelli, A. (2008)**.** Clathrin-dependent and independent endocytic pathways in tobacco protoplasts revealed by labelling with charged nanogold. J. Exp. Bot. **59**, 3051-3068.

Onelli, E., and Moscatelli, A. (2013). Endocytic pathways and recycling in growing pollen tubes. Plants doi:10.3390/plants2020211.

Parton, R.M., Fisher-Parton, S., Watahiki, M.K., and Trewavas. A. J. (2001). Dynamics of the apical vesicle accumulation and the rate of growth are related in individual pollen tubes. J. Cell Sci. **114**, 2685-2695.

Potocky, M., Elias, M., Profotova, B., Novotna, Z., Valentova, O., and Zarsky, V. (2003). Phosphatidic acid produced by phospholipase D is required for tabacco pollen tube growth. Planta **217**, 122-130.

Poulter, N.S., Vatovec, S., and Franklin-Tong, E. (2008) Microtubules are a target for self incompatibility signalling in *Papaver* pollen. Plant Physiol. **146**, 1358-1367.

Preuss, M.L., Serna, J., Falbel, T.G., Bednarek, S.Y., and Nielsen, E. (2004). The *Arabidopsis* Rab GTPase RabA4b localizes to the tips of growing root hair cells. Plant Cell **16**, 1589-1603.

Romagnoli, S., Cai, G., and Cresti, M. (2003). In vitro assays demonstrate that pollen tube organelles use kinesin-related motor proteins to move along microtubules. Plant Cell **15**, 251-69.

Samson, F., Donoso, A.J., Heller-Bettingher, I., Watson, D., and Himes R. H. (1979). Nocodazole action on tubulin assembly, axonal ultrastructure and fast axoplasmic transport. J. Pharm. Exp. Ther. **20**, 411-417.

Sanford, J.C., Smith, F.D., and Russell, J.A. (1993). Optimizing the biolistic process for different biological applications. Methods Enzymol. **217,** 483-509.

Schafer, D.A. (2002). Coupling actin dynamics and membrane dynamics during endocytosis. Curr. Opin. Cell Biol. **14**, 76-81.

Schneider, C.A., Rasband, W.S., and Eliceiri, K.W. (2012). NIH Image to ImageJ: 25 years of image analysis. Nature Methods **9**, 671-675.

Sharma, S., Ganesh, T., Kingstone, D.G.I., and Bane, S. (2007). Promotion of tubulin assembly by poorly soluble taxol analogs. Anal. Biochem. **360**, 56-62.

Snustad, D.P., Haas, N.A., Kopczak, S.D., and Silflow, C.D. (1992). The small genome of *Arabidopsis* contains at least nine expressed β-tubulin genes. Plant Cell **4**, 549-556.

Soldati, T. (2003). Unconventional myosins, actin dynamics and endocytosis: a ménage à trois? Traffic **4**, 358–366.

Steer, M.W., and Steer, J.L. (1989). Pollen tube tip growth. New Phytol. **111**, 323-358.

Szumlanski, A. L. and Nielsen, E. (2009) The Rab GTPase RabA4d Regulates Pollen Tube Tip Growth in *Arabidopsis thaliana*. Plant Cell **21**, 526-544.

Terasaka, O., and Niitsu, T. (1994). Kinesin localized in the pollen tube tips of *Pinus densiflora*. Jpn. J. Palynol. **40**, 1-6.

Tiezzi, A., Moscatelli, A., Cai, G., Bartalesi, A., and Cresti, M. (1992). An immunoreactive homolog of mammalian kinesin in *Nicotiana tabacum* pollen tube. Cell Motil. Cytoskel. **21**, 132-137.

Tirnauer, J.S., Grego, S., Salmon, E.D., and Mitchison, T.J. (2002). EB1–microtubule interactions in *Xenopus* egg extracts: role of EB1 in microtubule stabilization and mechanisms of targeting to microtubules. Mol. Biol. Cell **13**, 3614-3626.

Twell, D., Yamaguchi, J., and McCormick, S. (1990). Pollen-specific gene expression in transgenic plants: coordinate regulation of two different tomato gene promoters during microsporogenesis. Development **109**, 705-713.

Ueda, K., Matsuyama, T., and Hashimoto, T. (1999). Visualization of microtubules in living cells of transgenic *Arabidopsis thaliana*. Protoplasma **206**, 201-206.

Vaquez, R. J., Howell, B., Yvon, A-M.C., Wadsworth, P., and Cassimeris, L. (1997). Nanomolar concentration of Nocodazole alter microtubule dynamic instability in vivo and in vitro. Mol. Biol. Cell **8**, 973-985.

Viotti, C., Bubeck, J., Stierhof, Y.D., Krebs, M., Langhans, M., Van der Berg, W., van Dongen, W., Richter, S., Geldner, N., Takano, J., Jurgens, G., de Vries, S.C., Robinson, D.G., and Schumacher, K. (2010). Endocytic and secretory traffic in *Arabidopsis* merge in the Trans Golgi Network/Early endosome, an independent and highly dynamic organelle. Plant Cell **22**, 1344-1357.

Wang, H., Tse, Y.C., Law, A.H., Sun, S.S., Sun, Y.B., Xu, Z.F., Hillmer, S., Robinson, D.G., and Jiang, L. (2010). Vacuolar sorting receptors (VSRs) and secretory carrier membrane proteins (SCAMPs) are essential for pollen tube growth. Plant J. **61**, 826-838.

Wilcke, M., Johannes, L., Galli, T., Mayau, V., Goud, B., and Salamero, J. (2000). Rab11 regulates the compartmentalization of early endosomes required for efficient transport from early endosomes to the trans-golgi network. J. Cell Biol. **151**, 1207-1220.

Ye, J., Zheng Y., Yan, A., Chen, N., Wang, Z., Huang, S., and Yang, Z. (2009). *Arabidopsis* formin 3 directs the formation of actin cables and polarized growth in pollen tubes. Plant Cell **21**, 3868-3884.

Zerial, M. and McBride, H. (2001). Rab proteins as membrane organizer. Nat. Rev. Mol. Cell Biol. **2**, 107-117.

Zhao, Y., Yan, A., Feijo, J.A., Furutani, M., Takenawa, T., Hwang, I., Fu, Y., and Yang, Z. (2010). Phosphoinositides regulate clathrin-dependent endocytosis at the tip of pollen tubes in *Arabidopsis* and tobacco. Plant Cell **22**, 4031-4044.

Zonia, L., and Munnik, T. (2008). Vesicle trafficking dynamics and visualization of zones of exocytosis and endocytosis in tobacco pollen tubes. J. Exp. Bot. **59**, 861-873.

Figure 1

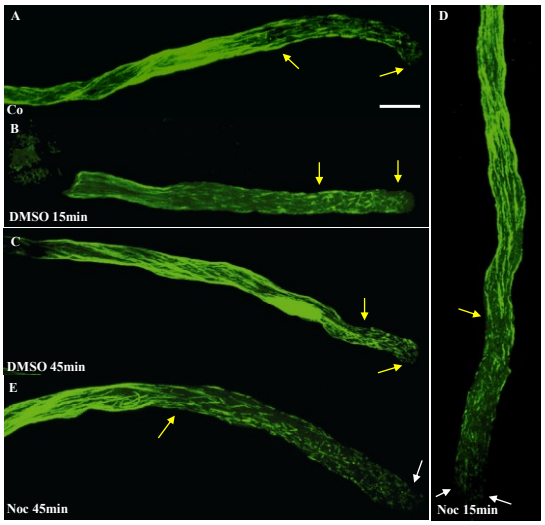

Fig. 1

Figure 2

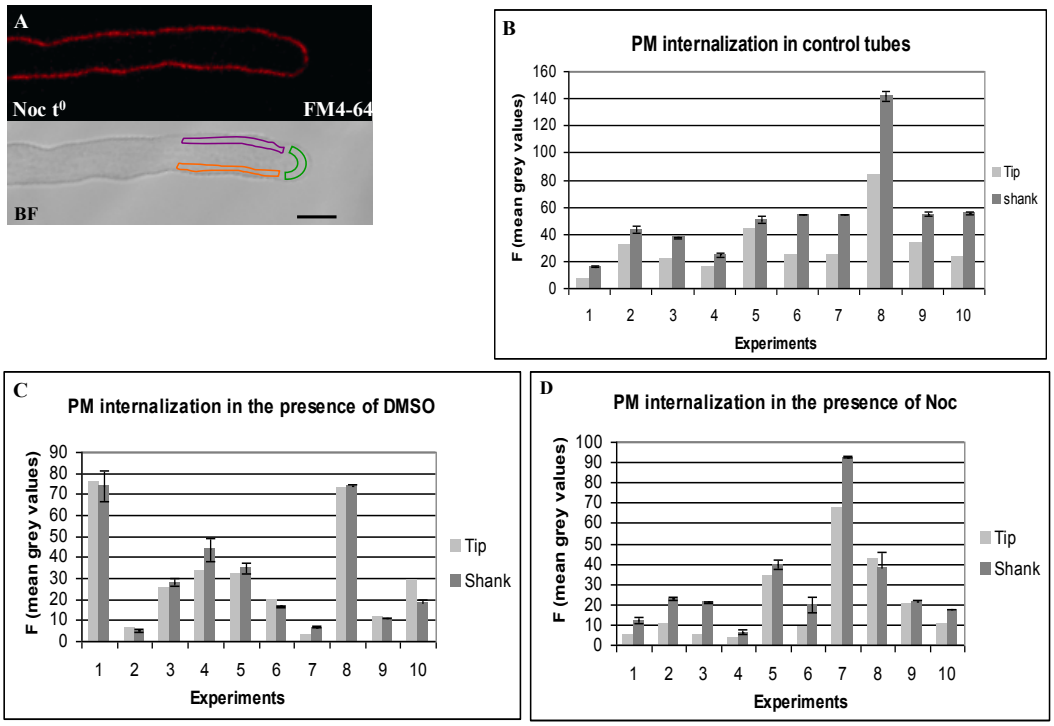

Fig. 2

Figure 3

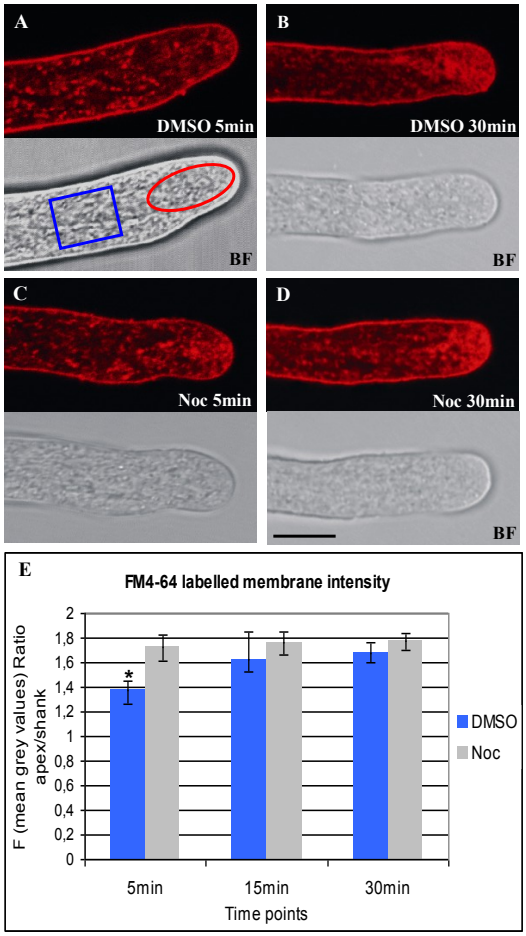

Fig. 3

Figure 4

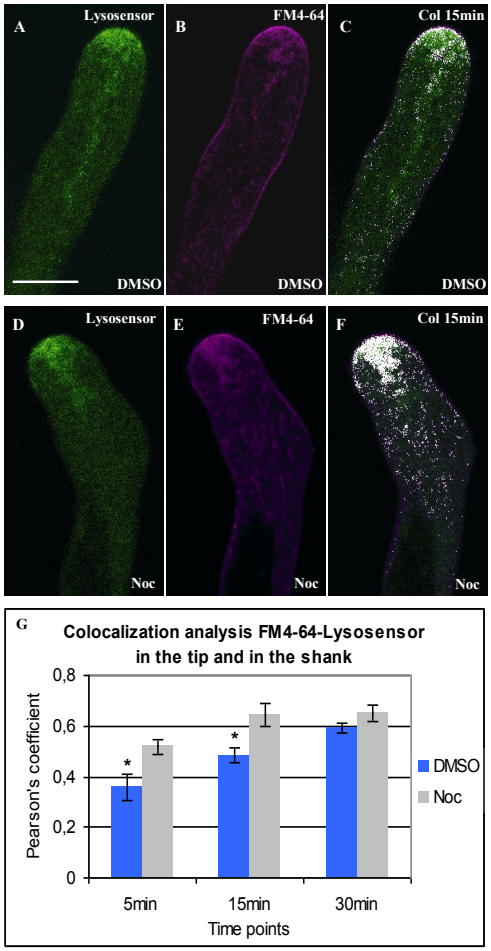

Fig. 4

Figure 5

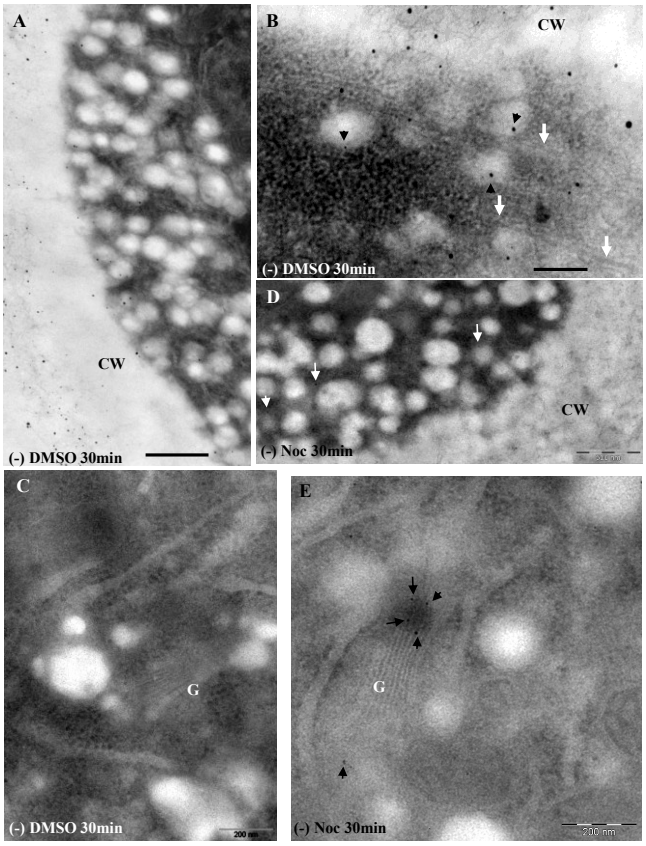

Fig. 5

Figure 6

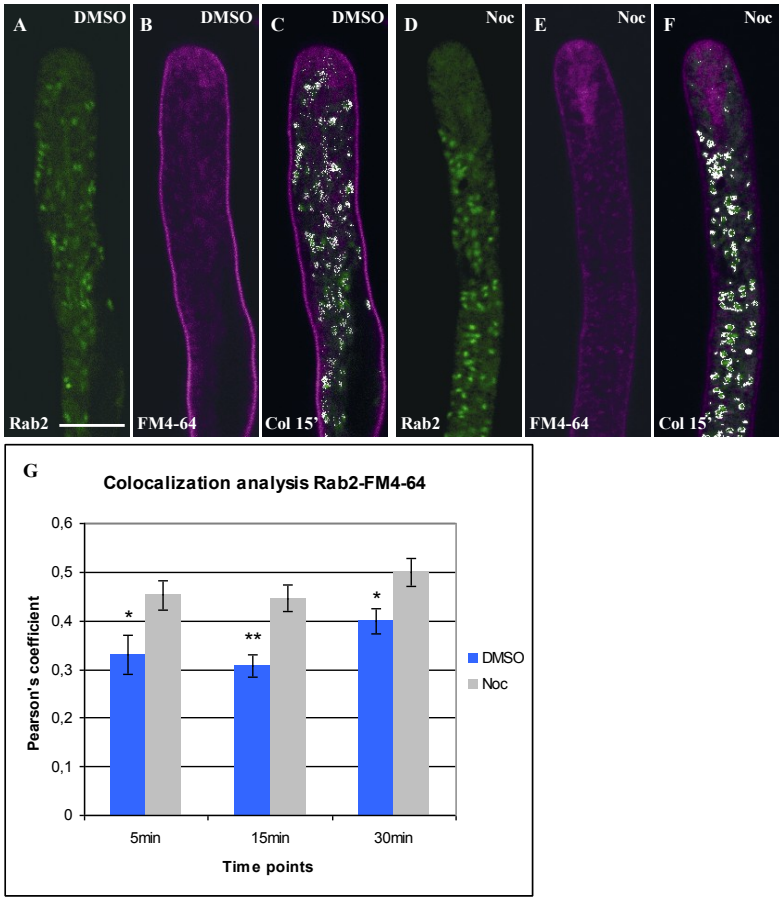

Fig. 6

Figure 7

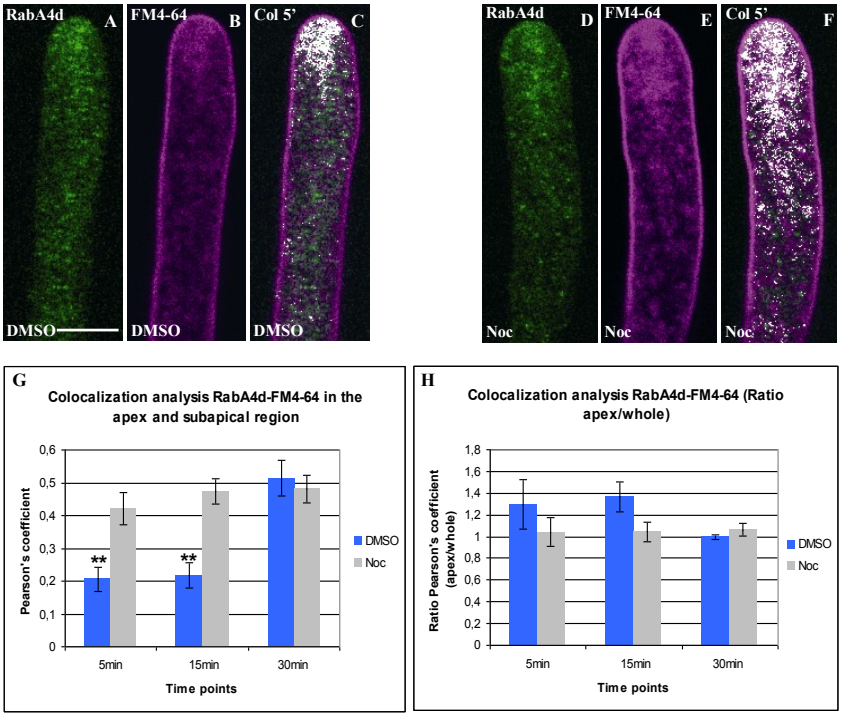

Fig. 7

Figure 8

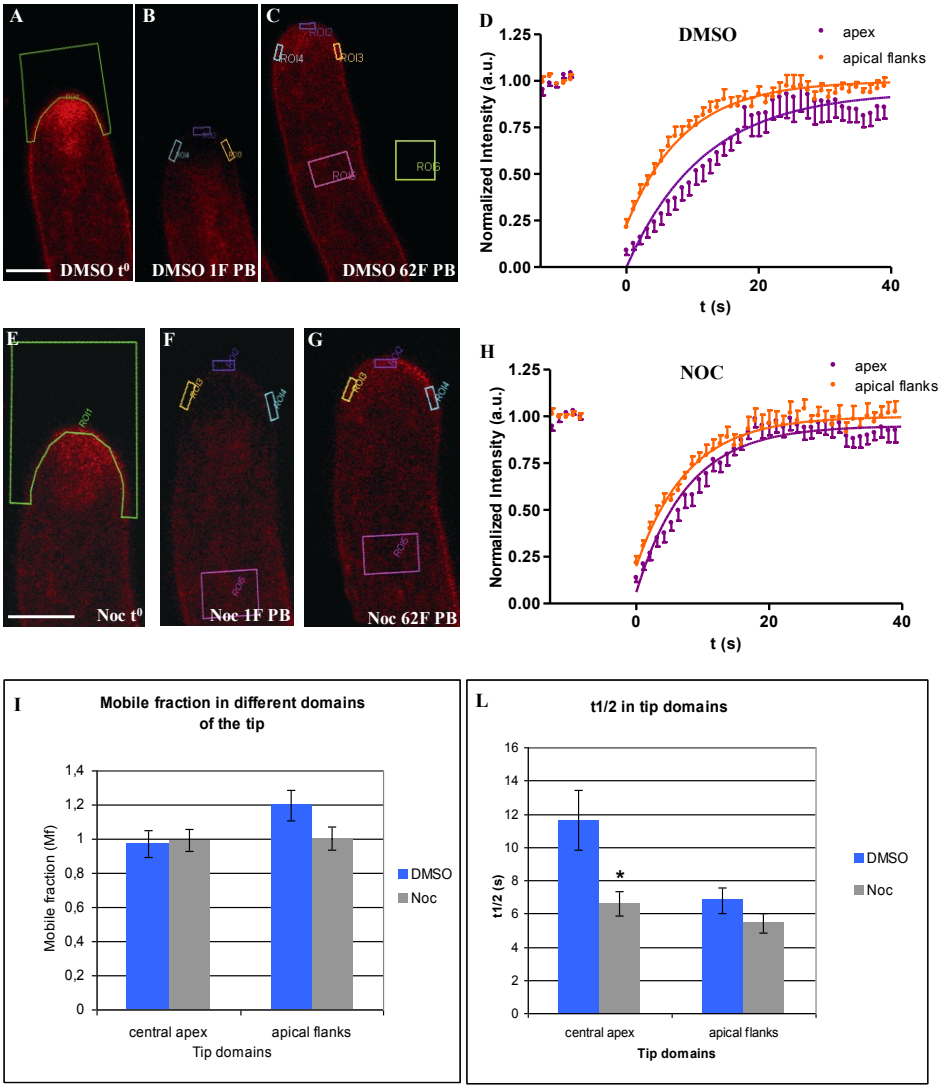

Fig. 8

Figure 9

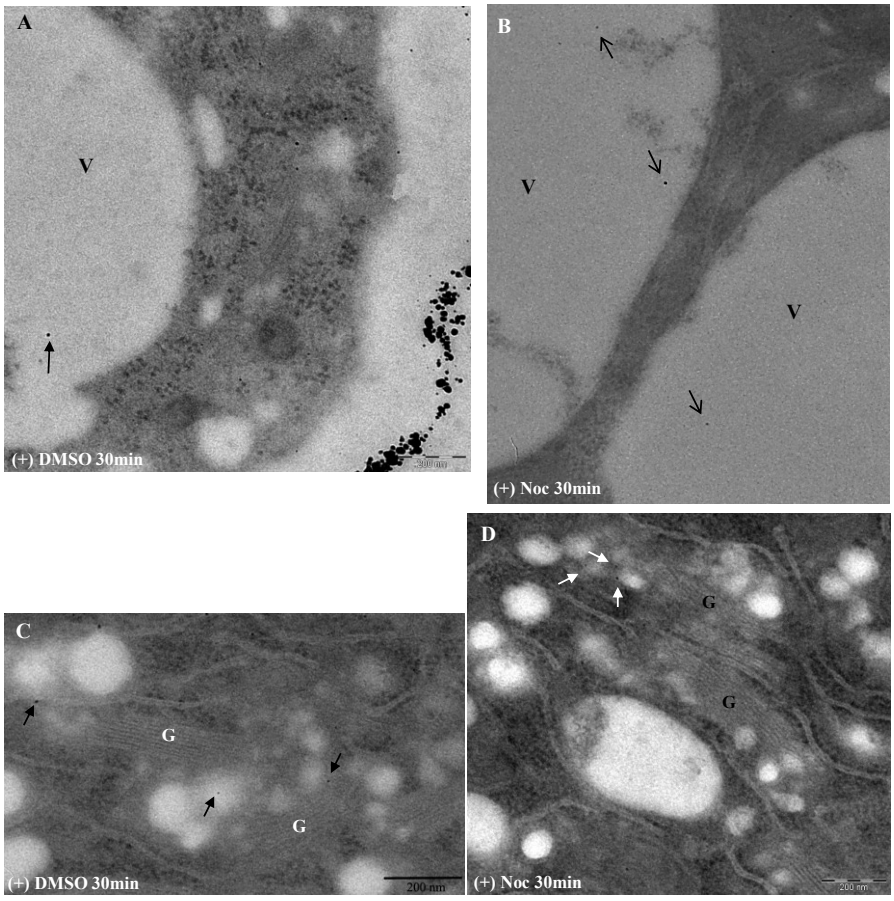

Fig. 9